Pacific–East Asian Teleconnection: How Does ENSO Affect East Asian Climate?*

BIN WANG, RENGUANG WU, AND XIOUHUA FU

Department of Meteorology and International Pacific Research Center,+ School of Ocean and Earth Science and Technology, University of Hawaii at Manoa, Honolulu, Hawaii

(Manuscript received 27 April 1999, in final form 22 June 1999)

ABSTRACT

Observational evidence is presented to show a teleconnection between the central Pacific and East Asia during the extreme phases of ENSO cycles. This Pacific–East Asian teleconnection is confined to the lower troposphere. The key system that bridges the warm (cold) events in the eastern Pacific and the weak (strong) East Asian winter monsoons is an anomalous lower-tropospheric anticyclone (cyclone) located in the western North Pacific. The western North Pacific wind anomalies develop rapidly in late fall of the year when a strong warm or cold event matures. The anomalies persist until the following spring or early summer, causing anomalously wet (dry) conditions along the East Asian polar front stretching from southern China northeastward to the east of Japan (Kuroshio extension).

Using atmospheric general circulation and intermediate models, the authors show that the anomalous Philippine Sea anticyclone results from a Rossby-wave response to suppressed convective heating, which is induced by both the in situ ocean surface cooling and the subsidence forced remotely by the central Pacific warming. The development of the anticyclone is nearly concurrent with the enhancement of the local sea surface cooling. Both the anticyclone and the cooling region propagate slowly eastward. The development and persistence of the teleconnection is primarily attributed to a positive thermodynamic feedback between the anticyclone and the sea surface cooling in the presence of mean northeasterly trades. The rapid establishment of the Philippine Sea wind and SST anomalies implies the occurrence of extratropical–tropical interactions through cold surge–induced exchanges of surface buoyancy flux. The central Pacific warming plays an essential role in the development of the western Pacific cooling and the wind anomalies by setting up a favorable environment for the anticyclone–SST interaction and midlatitude–tropical interaction in the western North Pacific.

1. Introduction

The East Asian monsoon system is one of the most active components of the global climate system. Climate variability in East Asia has notable impacts on both adjacent regions and the regions far away (Lau and Li 1984; Yasunari 1991; Lau 1992). El Niño–Southern Oscillation (ENSO) exhibits the greatest influence on the interannual variability of the global climate (Webster et al. 1998). The mature phase of ENSO often occurs in boreal winter and is normally accompanied by a weaker than normal winter monsoon along the East Asian coast (Zhang et al. 1996; Tomita and Yasunari 1996; Ji et al. 1997). Consequently, the climate in southeastern China and Korea is warmer and wetter than normal during ENSO winter and the ensuing spring (Tao and Zhang 1998; Kang and Jeong 1996).

Figure 1 shows correlation maps of the monthly Climate Prediction Center (CPC) merged analysis of precipitation (CMAP) with reference to the SST anomaly in the Niño-3.4 region (5°S–5°N, 120°–170°W). The CMAP data are derived from various sources of satellite observations and station rain gauge data (Xie and Arkin 1997). To alleviate the effects of inhomogeneous seasonal distributions of precipitation on the correlation analysis, we used normalized monthly precipitation anomalies (the anomalous monthly precipitation divided by the corresponding monthly standard deviations). A positive correlation means increased rainfall when the Niño-3.4 SST is above normal. The warm (cold) peak in the Niño-3.4 region tends to occur toward the end of the calendar year (Rasmusson and Carpenter 1982; also Fig. 3). Therefore, the correlation at lag 0 represents the precipitation anomalies in the boreal winter, while the lag-3- and lag-6-month correlation maps reflect, respectively, the rainfall anomalies in March and June after the peak ENSO.

The precipitation anomalies associated with global

* School of Ocean and Earth Science and Technology Publication Number 5010 and IPRC Publication Number 16.

+ The International Pacific Research Center is partly sponsored by the Frontier Research System for Global Change.

Corresponding author address: Prof. Bin Wang, Department of Meteorology and IPRC, University of Hawaii at Manoa, 2525 Correa Road, Honolulu, HI 96822.
E-mail: bwang@soest.hawaii.edu

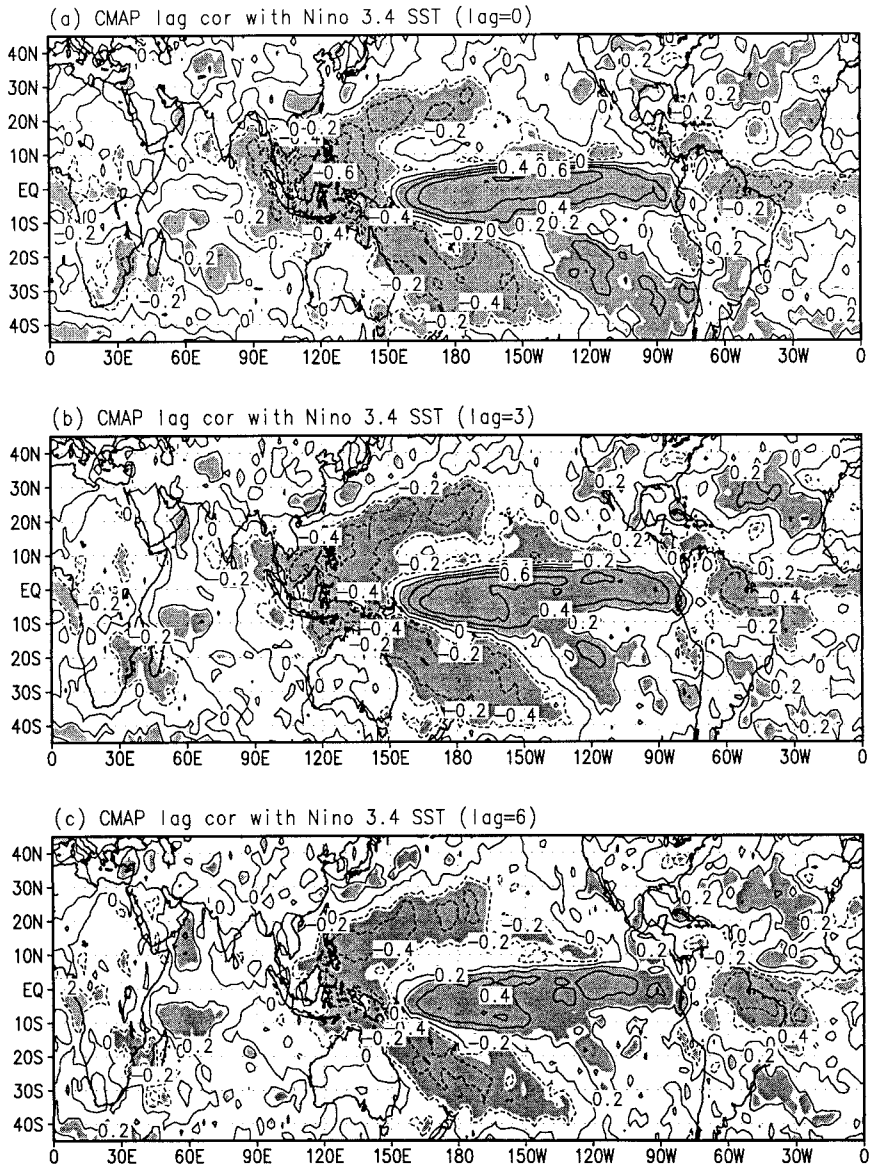

FIG. 1. Correlation maps of the CMAP (Xie and Arkin 1997) rainfall with reference to Niño-3.4 SST (5°S–5°N, 120°–170°W) anomalies (SSTAs) at (a) lag = 0 (simultaneous), (b) lag = +3 (rainfall anomalies lag Niño-3.4 SSTA by 3 months), and (c) lag = +6 (rainfall anomalies lag Niño-3.4 SSTA by 6 months). The data used are 3-month running mean anomalies during 1979–96. The shaded regions denote correlation coefficients significant at 95% confidence level.

SST anomalies during the mature phase of ENSO exhibit a striking dipole with a dry polarity being located at the Maritime Continent and a wet polarity in the equatorial eastern–central Pacific (Fig. 1). From these polarity centers, anomalous dry and wet bands emanate poleward and eastward toward the extratropics. The anomalously dry zone in the western Pacific exhibits a horseshoe pattern. Note that the equatorial rainfall anomalies have a zonal wavenumber-2 structure. A secondary dry (wet) dipole pattern is discernible outside of the Indonesia–Pacific region in all three lag-correlation maps. The large-scale features in the tropical and subtropical precipitation anomalies (Fig. 1) are consistent with the results presented by Ropelewski and Halpert (1987, 1989). Differences are found in the extratropics and on regional scales possibly due to different record lengths of the datasets and to the nonsteadiness and regionality of the atmospheric response to the lower boundary forcing.

Noticeable positive precipitation anomalies occur along the East Asian polar front from southern China via the East China Sea to the Kuroshio extension region during winter and the following spring/early summer (Figs. 1a,b,c). This concurs with and extends the results

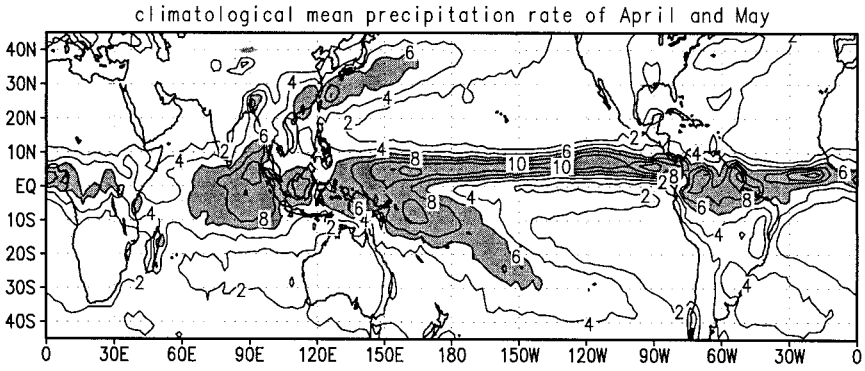

FIG. 2. Climatological mean precipitation rates for the period from 1 Apr to 31 May. The data come from CMAP. The precipitation rates > 6 mm day^{-1} are shaded.

of the previous studies of ENSO impacts on regional climates in southern China (Tao and Zhang 1998), Taiwan (Wang and Hwu 1994), and Korea (Kang and Jeong 1996). It is important to note that the increased rainfall from March to June coincides with the local rainy seasons in those regions. This can be seen from Fig. 2, which shows a prominent rain band along the East Asian polar front in April and May. This rainband is nearly quasi-stationary from March to May and then ''jumps'' rapidly northward, becoming the Meiyu (Baiu) in mid-June. As such, the anomalous rainfall occurring in this season considerably modifies the characteristics of a normal rainy season. Thus, ENSO exerts a significant impact on the annual rainfall in the East Asian spring polar front and possibly the subsequent Meiyu (Baiu) front (e.g., Fu and Teng 1988).

The pioneering works of Bjerknes (1966, 1969) reveal a teleconnection between the equatorial central Pacific warming and the North Pacific extratropical circulation anomalies. He interpreted the teleconnection as resulting from changes in the Hadley circulation and associated energy and momentum transport. The downstream effects of ENSO on North American climate have been referred to as the Pacific–North American (PNA) teleconnection (Wallace and Gutzler 1981; Horel and Wallace 1981) and explained by forced Rossby wave trains (Hoskins and Karoly 1981) and barotropic instability of the midlatitude westerlies (e.g., Simmons et al. 1983). The wave trains and instability are excited by the upper-tropospheric divergence associated with the enhanced convection in the equatorial central Pacific. A large number of papers have been published to explore the cause and predictability of the PNA teleconnections.

How can the eastern–central Pacific warming affect the ''upstream'' (with respect to the direction of the midlatitude westerlies) climate in the East Asia? This has not been well understood. Based on a diagnostic analysis of the 1986/87 and 1991/92 events, Zhang et el. (1996) speculate that the effects of the El Niño events on the East Asian summer monsoon are felt through the variation of convective activity over the equatorial western Pacific. The warming in the eastern Pacific suppresses convection in the equatorial western Pacific. The latter then influences the monsoon circulation over the tropical western Pacific and East Asia. Note, however, that the mature phases of the 1986/87 and 1991/92 events occurred, respectively, in boreal summer and winter. The climatological mean state in the western Pacific exhibits a sharp contrast between summer and winter. It is not clear how the East Asian anomalies can be generated in remarkably different mean states. The relationship between SST anomalies and summer rainfall in East Asia is a very controversial issue. The regions where SST anomalies have been identified as influential to the East Asian summer monsoon include the Kuroshio currents, the western Pacific warm pool, the eastern equatorial Pacific, the South China Sea, and the Indian Ocean (e.g., Huang and Lu 1989; Shen and Lau 1995; Nitta and Hu 1996). These anomalies are, to a certain degree, all related to ENSO. Yet, significant correlations could not be found between the eastern Pacific SST anomalies and the East Asian summer monsoon (e.g., Chen et al. 1992). The divergence of these results suggests that the year-to-year variability of the East Asian summer monsoon is probably affected by very complex air–sea–land interaction and tropical–extratropical interaction. ENSO is only one of the major factors among others such as Tibetan Plateau heating, Eurasian snow cover, and polar ice coverage.

The purpose of the present study is to address the question of how the ENSO anomalies can affect the East Asian monsoon during and after their mature phases from boreal winter to the early summer of the following year. Emphasis is placed on understanding the physical processes that underlie the establishment of the teleconnection between the eastern–central Pacific and East Asia. For this purpose, we first document the observed structures (section 3) and evolution (section 4) of the Pacific–East Asian teleconnection during the major Pacific warm and cold episodes. This is followed by an investigation of the roles of tropical Pacific SST anomalies in generating atmospheric anomalies by means of numerical experiments (section 5). Section 6 discusses the causes of the rapid establishment and notable per-

sistence of the wind and SST anomalies in the western North Pacific. The last section summarizes our findings along with a discussion of some of the key issues that call for future investigation.

2. Data and analysis procedure

The primary dataset used is the National Centers for Environmental Prediction–National Center for Atmospheric Research (NCEP–NCAR) global atmospheric reanalysis dataset covering a 41-yr period from January 1958 to December 1998. A detailed description of the data assimilation system that produces this dataset is given by Kalnay et al. (1996). The data assimilation system was based on the global forecast model that was implemented operationally at NCEP in January 1995. The observational database includes considerable amounts of data that were not available in real time. A spectral statistical interpretation and a three-dimensional variational analysis method were adapted for data assimilation. We used monthly mean data on standard pressure surfaces gridded onto a 2.5° latitude–longitude grid. In addition, we use monthly mean SST, sea level pressure, and surface winds, which are derived from the Comprehensive Ocean–Atmosphere Data Set (COADS; Woodruff et al. 1987), as a complementary dataset for checking the results derived from the reanalysis data and for providing data for the period prior to January 1958 when they are needed.

We focus on the most prominent basinwide warm and cold episodes in the tropical Pacific (for simplicity, referred to as major El Niño and La Niña episodes, respectively). These major El Niño and La Niña episodes are defined using 3-month running mean Niño-3.4 SST anomalies and the following two criteria. (a) The maximum (minimum) SST anomaly exceeds one standard deviation (about 1.0°C), and (b) SST anomalies exceeding 0.5°C persist for at least 8 months. According to these criteria, six major El Niño (1957/58, 1965, 1972, 1982/83, 1991/92, 1997/98) and five major La Niña (1970/71, 1973/74, 1975/76, 1984/85, and 1988/89) episodes are identified for the period from 1950 to 1998. The 1986/87 warm episode meets the above criteria, but its phase evolution with respect to the annual cycle is at odds with all others. In the composite study, we have to exclude it but will discuss that special case separately in the last section.

Figure 3 displays the time series of Niño-3.4 SST anomalies around the warm (cold) peaks of the major El Niño (La Niña) events. The time window spanning 23 months is centered on December of the year during which warm (cold) events mature. Note that the maximum (minimum) Niño-3.4 SST anomalies for each warm (cold) episode occurred during the calendar months from November to January. This indicates a robust tendency for mature phases of warm and cold episodes (defined by Rasmusson and Carpenter 1982) to occur toward the end of the calendar year, although

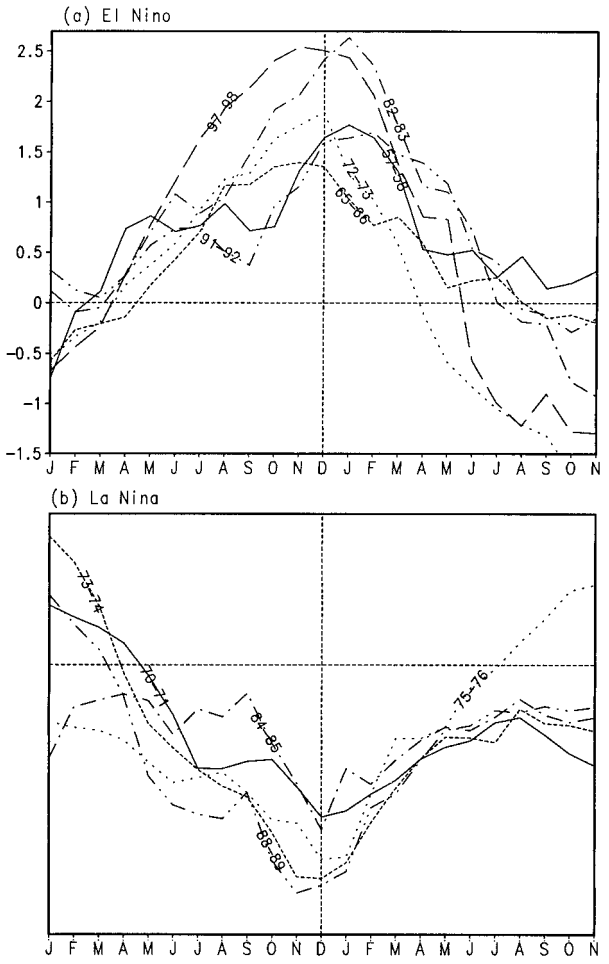

FIG. 3. Evolution of monthly mean Niño-3.4 SST anomalies (°C) from Jan of the ENSO development year to Nov of the following year for (a) the six warmest and (b) the five coldest episodes during the period 1950–98.

the characteristics of the *onset* phases of ENSO cycles have experienced drastic changes in the late 1970s (Wang 1995a; Torrence and Webster 1998).

Because of this tight phase locking to the annual cycle, it is meaningful to make a composite analysis. The composites can be made based on the evolution of the Niño-3.4 SST anomalies. For simplicity, the composites for the selected six major warm and six major cold episodes will be termed as the composite warm and cold events, respectively. We will emphasize only the contrasting features between the composite warm and cold events that are statistically significant through a *t* test at a 95% confidence level.

3. The structure of the Pacific–East Asian teleconnection

a. Lower-troposphere anomalies

To illustrate the common characteristics of the lower-tropospheric anomalies during warm (cold) mature

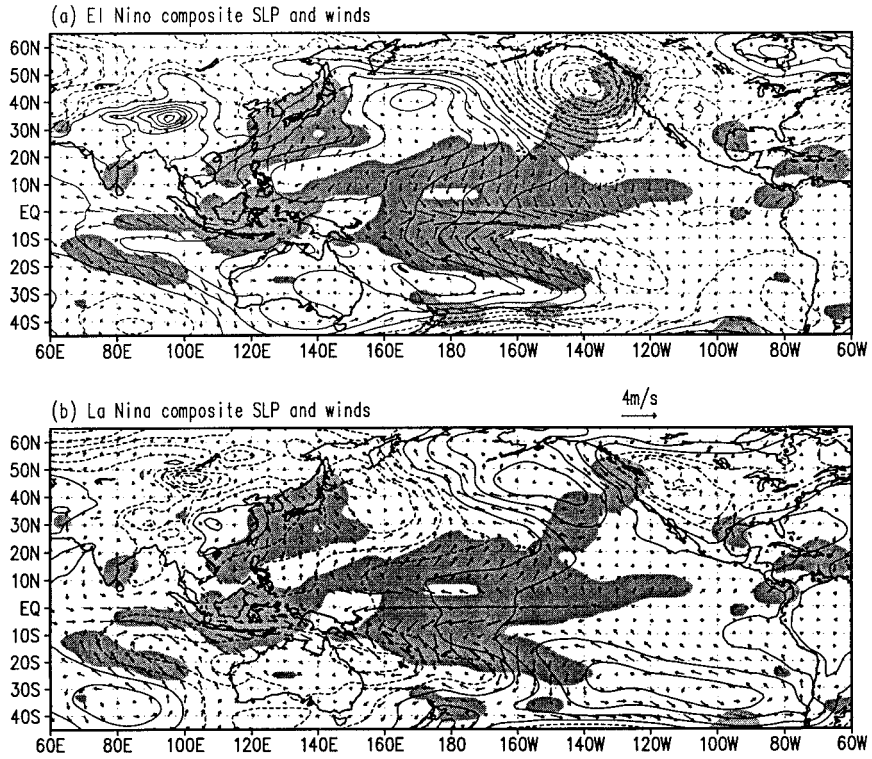

FIG. 4. Composite 3-month mean surface wind and sea level pressure anomalies around the peaks of (a) the six warmest and (b) the five coldest episodes illustrated in Fig. 3. The shaded areas indicate regions where the difference in surface winds between the warm and cold composite are statistically significant at 99% confidence level by *t* test. The contour interval for sea level pressure anomalies is 0.5 hPa. The vectors between the panels indicate the scale for wind anomalies.

phases of ENSO cycles, we present, in Figs. 4a and 4b, composite maps of sea level pressure and surface wind anomalies around the peaks of the major El Niño and La Niña episodes, respectively. Since the cold and warm composites largely mirror each other, our description and discussion will focus on the warm composite (Fig. 4a).

In response to the basinwide warming, a pair of anomalous surface anticyclones form over the western Pacific, having some degree of symmetry about the equator. The massive western North Pacific anticyclone contains two separate centers. One is located over the Philippine Sea and well within the Tropics. Another anomalous anticyclone center (40°N and 170°E) is found in the midlatitude over the Kuroshio extension. Anomalous southwesterlies prevail to the northwest of the Philippine Sea anticyclone, implying weaker than normal northeastly winter monsoon along the East Asian coast or a warmer than normal winter in that region. Downstream of the midlatitude anticyclonic anomalies is an anomalous low centered around 45°N and 140°W. The associated anomalous southerlies transport warm and moist air toward the west coast of North America. This northward transport along with the ascending motion in front of the cyclone induces a wetter than normal climate along the coastal areas of California (Ropelewski and Halpert 1996). The anomalous southerlies also cause coastal ocean warming by suppressing the upwelling off California.

The western North Pacific (WNP) anticyclone is a key system that bridges the eastern-central Pacific warming and the East Asian winter monsoon. The equatorial central Pacific warming induces a nearby cyclonic response to the northwest (southwest) of the warming. This is manifested by the equatorward flows associated with the equatorial westerly anomalies near the dateline, which exhibit strong cyclonic vorticities (Fig. 4a). In terms of streamfunction, which has a sign opposite to vorticity, a negative (positive) anomaly center resides on the north (south) of the equator (Fig. 5a). This antisymmetric anomalous streamfunction pattern indicates cyclonic rotational flows residing at each side of the equator—a Rossby wave response to the anomalous equatorial central Pacific heating (Matsuno 1966; Gill 1980) associated with the ENSO warming. The northeasterly anomalies induced by the central Pacific warming are located in the front (east) of the Philippine Sea anticyclone. On the other hand, the weak East Asian winter monsoon manifests itself as southwesterly anomalies along the margin of the East Asian continent. These

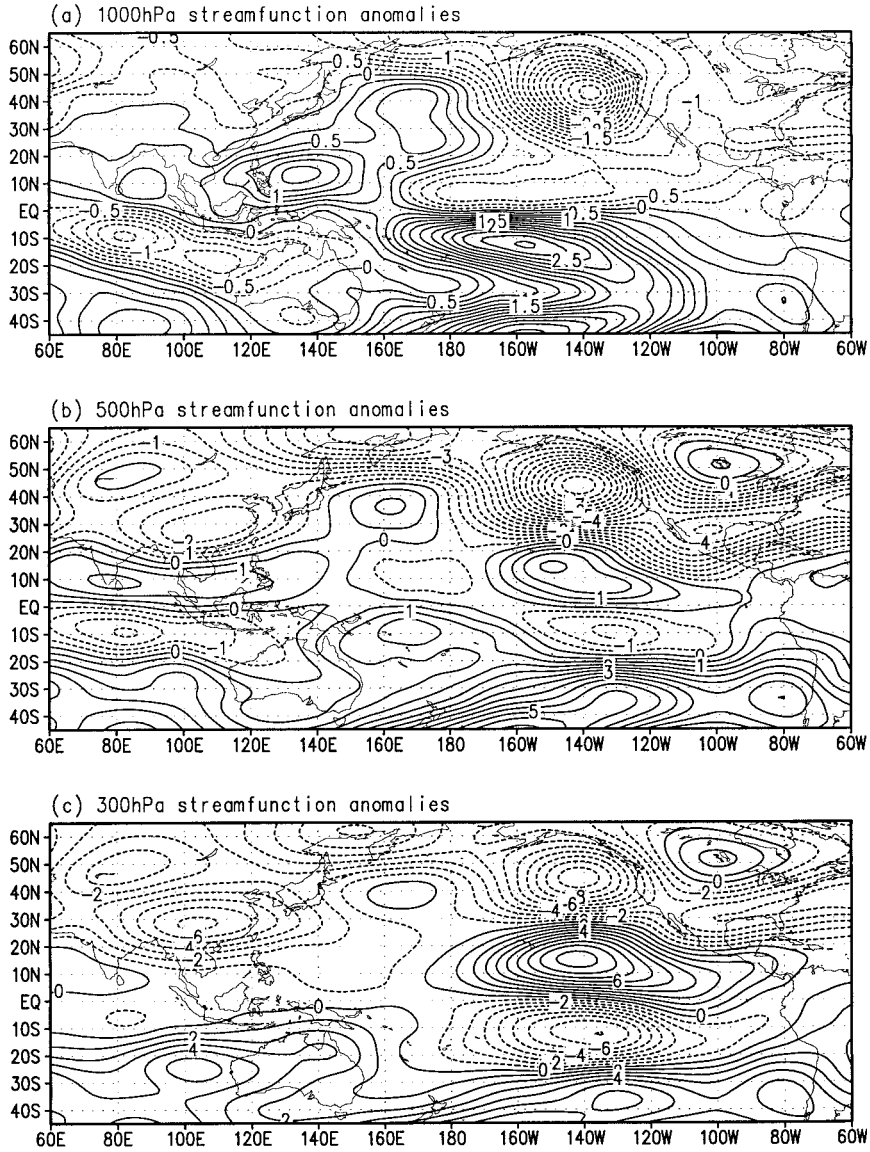

FIG. 5. Composite 3-month mean streamfunction anomalies at (a) 1000, (b) 500, and (c) 300 hPa around the peaks of the six warmest ENSO events shown in Fig. 3 (10^{-6} m^2 s^{-1}).

southwesterly anomalies are located in the rear (west) of the Philippine Sea anticyclone. In this sense, the Philippine anticyclone bridges the warming in the equatorial central Pacific and the weak East Asian winter monsoon. The central Pacific cyclonic vorticity, the WNP anticyclone, and the northeast Asian cyclonic vorticity comprise a surface vorticity wave pattern that starts from the central Pacific and extends poleward and westward to East Asia. This vorticity wave pattern can be better recognized from the surface streamfunction anomaly fields shown in Fig. 5a. We refer to this pattern as the Pacific–East Asian teleconnection.

The emanation of the vorticity waves is accompanied by sandwiched SST anomalies (the central Pacific warming, the western Pacific cooling, and the warming in the East Asian marginal seas) (Fig. 6a). The alternative occurrence of the cyclonic–anticyclonic–cyclonic vorticity pattern and the warm–cold–warm pattern are an indication and a possible result of the air–sea interaction in the western Pacific. As will be discussed in the next two sections, the SST anomalies and the wind vorticity patterns are generated by the equatorial central Pacific warming. The central Pacific is a source region for such teleconnection patterns.

b. The vertical structure

The Pacific–East Asian teleconnection is primarily confined to the lower troposphere. This is evident by inspecting Fig. 5, which displays anomaly streamfunc-

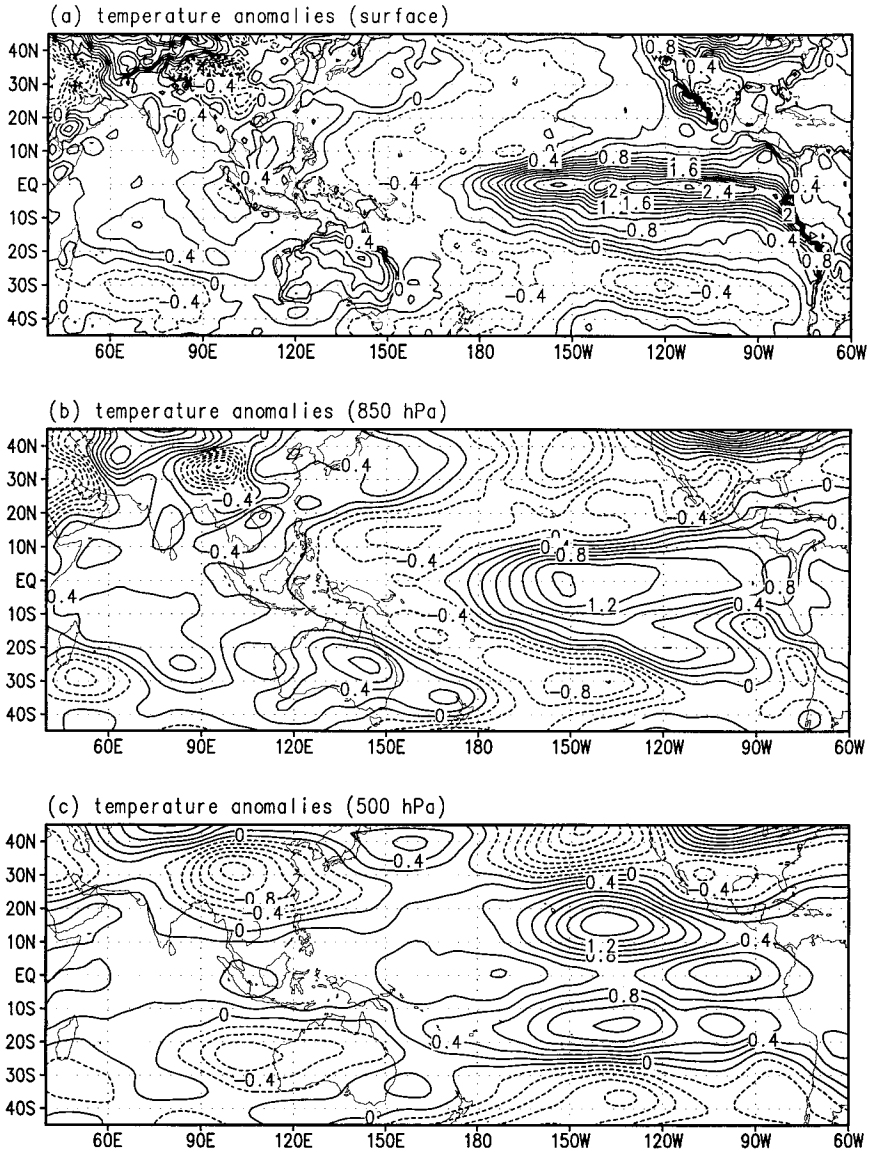

FIG. 6. Composite 3-month mean anomalies of the (a) sea (land) surface temperature and air temperature at (b) 850 and (c) 500 hPa around the peaks of the six warmest events shown in Fig. 3 (°C).

tions for the composite warm event at different vertical levels. The western North Pacific anticyclone, which bridges the warming in the equatorial central-eastern Pacific and the East Asian monsoon, is strongest at the surface and decays upward. In the midtroposphere, the WNP anticyclone remains evident but almost disappears at 300-hPa level. Note that the massive surface anticyclone exhibits two centers with the principal one in the Philippine Sea. The Philippine Sea anticyclone is primarily baroclinic, while the midlatitude portion of the anticyclone contains a considerable barotropic component. This suggests that the Philippine Sea anticyclone is likely stimulated by anomalous convective latent heating, which is greatest in the middle troposphere (hence the induced circulation is dominated by the lowest baroclinic mode). On the other hand, the anticyclone over the Kuroshio extension is likely associated with dynamical instability of the westerly jet. The intensity and location of the midlatitude portion of the WNP anticyclone displays large variability from event to event.

In the middle and upper troposphere (500 and 300 hPa), the Pacific–North American teleconnection pattern (Bjerknes 1969; Horel and Wallace 1981) and its Southern Hemisphere counterpart dominate. Over the Asian continent, a notable cyclonic anomaly occurs in Southeast Asia. Along the southern flank of the Southeast Asian low, an enhanced westerly jet extends northeastward from the Bay of Bengal all the way to Japan. These

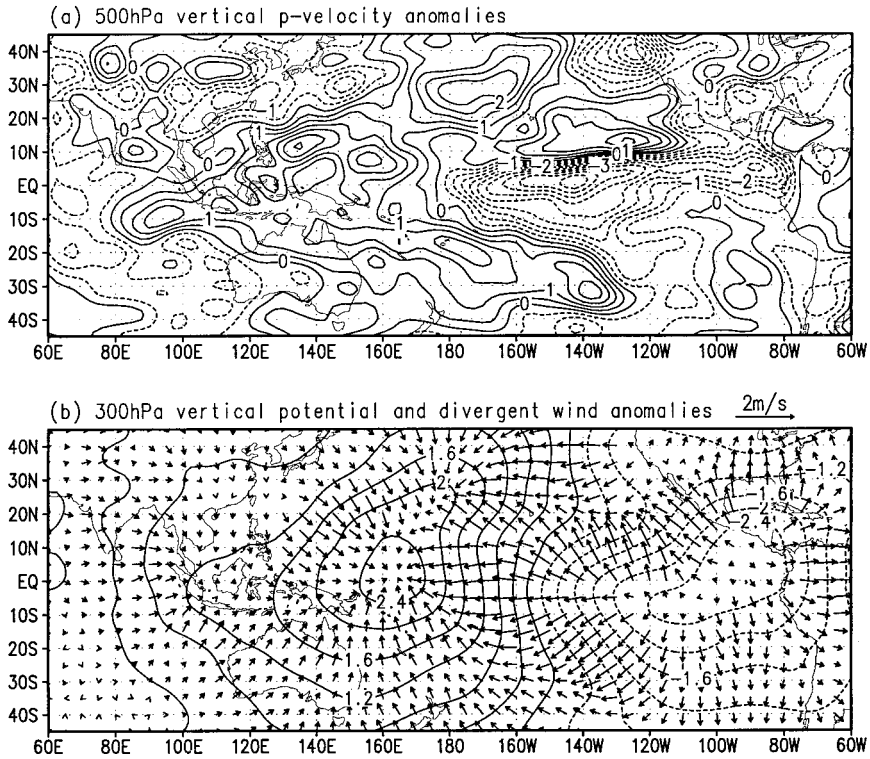

FIG. 7. Composite 3-month mean (a) 500-hPa vertical pressure velocity anomalies (10^{-2} Pa s^{-1}) and (b) 300-hPa velocity potential (10^{-6} m^2 s^{-1}) and divergent winds around the peaks of the six warmest events shown in Fig. 3. The divergent winds are calculated from the velocity potential. The wind scale is given at the upper right corner.

upper-level circulation anomalies favor warmer and wetter than normal weather along the East Asian polar front.

In the boundary layer (from the surface to 850 hPa), the air constituting the WNP anticyclonic anomaly is colder than normal to the east of the anticyclonic ridge, while it is warmer than normal to the west of the ridge (Figs. 6a,b). The 850-hPa temperature anomalies closely follow the SST anomalies, reflecting the influences from below by in situ surface heat exchange. In the western North Pacific, the amplitudes of the 850-hPa temperature anomalies are comparable to those at the surface, suggesting that the turbulent mixing in the boundary layer is very effective. This is because the cold northeasterly winter monsoon blowing over a warm ocean surface creates unstable stratification that favors vigorous upward buoyancy flux. Note that the lower-tropospheric temperature anomalies reverse their signs in the middle troposphere (Fig. 6c) because of the adiabatic warming induced by the large-scale sinking motion as shown in Fig. 7a.

The vertical thermal structure in the eastern Pacific is different. The warm anomalies weaken significantly as one progresses upward through the boundary layer (Figs. 6a,b). In the midtroposphere, two warm centers reside on each side of the equator around 140°W. The upper-tropospheric warming bears a similar pattern (figure not shown). The mid- and upper-tropospheric warming is likely a result of adiabatic descent compensating the equatorial ascent caused by the sea surface warming. This suggestion, however, is only partially supported by the composite vertical motion (Fig. 7a). The warming coincides well with the descent in the North Pacific, but not in the South Pacific. Lack of observations in the open ocean, especially in the southeast Pacific, makes the results less trustworthy.

The anomalous vertical motion at 500 hPa shows a pattern that is dynamically coherent with precipitation anomalies (Fig. 1a). Anomalous upward motions are found in the equatorial central Pacific and the East Asian polar frontal zone, whereas anomalous sinking motion occurs in between. From the equatorial central Pacific to East Asia, the vertical motion anomalies are also coherent with surface pressure anomalies. Over and to the east of the surface anticyclone sinking motion prevails, while in the rear of the anticyclone and the regions of cyclonic vorticity prevails anomalous ascent. Regardless of the patchy structure of the vertical velocity, in the western Pacific the downward motion evidently overlays surface cooling with a slight westward shift in the phase, similar to the phase shift of the surface anticyclone to negative SST anomalies.

The large-scale features of the anomalous vertical motion at 500 hPa are consistent with the upper-tropo-

spheric velocity potential (Fig. 7b). The latter are characterized by a dipole pattern with a convergence center in the eastern Philippine Sea and a divergence center above the equatorial eastern Pacific. Other minor divergence centers are discernible near the western coast of the United States and the East China Sea, coincident with enhanced upward motion in those regions (Fig. 7a). The strongest anomalous divergent winds concentrate over the central Pacific with a slight bias to the Northern Hemisphere. The upper meridional divergent flows between the Maritime Continent and East Asia are very weak, suggesting that the local meridional circulation in this region probably plays a minor role in coupling the equatorial heat anomalies over the Maritime Continent with the variation of the westerly jet over the East Asia. In other words, although ENSO induces an eastward shift of the equatorial heat source, it is not evident that the eastward shift of the equatorial heat source affects the midlatitude East Asian monsoon by altering the local meridional circulation.

4. Establishment and persistence of the Pacific–East Asian teleconnection

To understand the mechanisms behind the formation and maintenance of the Pacific–East Asian teleconnection, it is necessary to examine its detailed evolution. For convenience, we focus on the major warm episodes, although figures will include major cold episodes as well (e.g., Fig. 9b). To a large degree, the major cold episodes evolve in a manner resembling the warm episodes except with anomalies of opposite signs.

To illustrate the evolution of the WNP wind and SST anomalies, we present, in Fig. 8, the monthly mean surface wind and SST anomalies in the tropical Pacific during the mature phase of the 1982/83 warm event. Over the western North Pacific, the surface wind anomalies changed suddenly from cyclonic to anticyclonic in November of 1982. In December, the WNP anticyclone rapidly intensified and extended equatorward. Concurrently, the SST decreased rapidly in front of the anomalous anticyclone, reaching a minimum SST anomaly of -0.7°C. After the anomalous anticyclone developed, it remained and expanded eastward throughout the winter and the following spring. The cooling associated with the anticyclone also persisted and expanded slowly eastward along 10°–20°N.

The scenario described in Fig. 8 is common for major El Niño episodes. Figure 9 shows the evolution of sea level pressure anomalies over the Philippine Sea for each major warm and cold episode in comparison with the Niño-3.4 SST anomalies. One of the conspicuous features is that the *rapid* rise (drop) of pressure over the Philippine Sea often occurs in late fall and early winter. In most episodes, the establishment of the Philippine Sea anomalies leads the warm (cold) peak by 1–3 months. This important feature can also be seen from the composite evolution depicted in Fig. 10. Another noticeable feature is that the pressure anomalies normally persist for one to two seasons after their establishment. The peak pressure anomalies tend to lag corresponding SST anomalies. This feature agrees with the finding of Wang (1995b) that the sea level pressure (SLP) anomalies in the western North Pacific have a maximum positive correlation with the central Pacific warming at a lag of 3 months. The persistence is obvious for both the composite and individual episodes (Figs. 9 and 10).

Accompanying the eastern-central Pacific warming, cooling occurs over the western North Pacific (Fig. 6a). To reveal the evolution of the SST and wind anomalies in the off-equatorial Pacific, we present, in Fig. 11, a set of composite longitude–time diagrams across the North Pacific for atmospheric and SST anomalies associated with the major warm events. In theory (Gill 1980), the anticyclone (as a Rossby wave response) should occur to the northwest of the SST cooling. Indeed, the observations support the theory (Figs. 4a and 6a). To better reflect this phase relationship, in Fig. 11, we display SST anomalies averaged between 5° and 15°N, along with SLP and vertical motion anomalies averaged between 10° and 20°N (i.e., SLP anomalies are slightly to the north of the cooling). The cooling starts to exceed -0.4°C about 2 months prior to the warm peak along 150°E (Fig. 11a). Thereafter it maintains its strength (below -0.4°C) until about 4 months after the warm peak. Notice that the SLP over the Philippine Sea (120°–160°E) increases from below to above normal about 2 months prior to the warm peak (Fig. 11b). Nearly concurrent with the rise of the SLP, the 500-hPa anomalous vertical motion reverses sign (Fig. 11c). In accordance with the pressure changes in the Philippine Sea, the anomalous zonal winds to the south of the Philippine Sea between the equator and 10°N reverse from westerly to easterly anomalies (Fig. 11d).

If we focus on the longitudinal sector between 140° and 180°E where the maximum SLP and minimum SST anomalies occur, a nearly simultaneous rising of the SLP and cooling of the sea surface are evident. Note that the maximum pressure (anticyclonic) anomalies are located about 20° longitude to the west of the maximum cooling. Both the negative SST and positive SLP anomalies show a coherent tendency of slow eastward extension. These features suggest a coupling between wind and SST anomalies in the western North Pacific. A similar coherent evolution of the anomalies of the meridional component of surface wind, SST, and surface humidity along 30°–35°N was found using observations obtained by spaceborne sensors (Liu et al. 1998).

5. Roles of tropical SST anomalies in forcing Philippine Sea anticyclones

The massive western North Pacific anticyclonic anomalies that occur during a mature phase of the Pacific warming cover both the Tropics and extratropics.

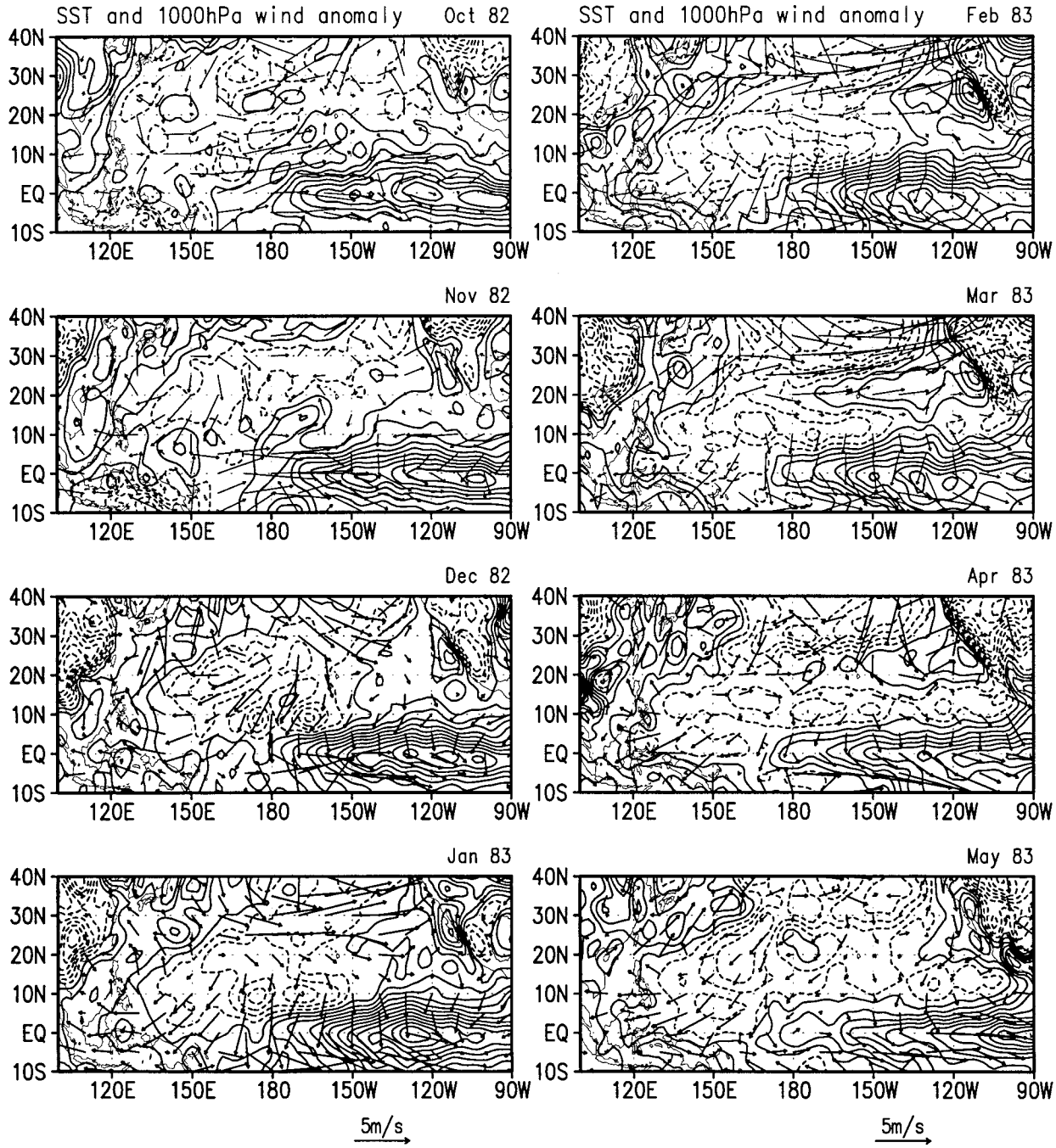

FIG. 8. Monthly mean anomalies of surface winds and SST (contour interval 0.2°C) from Oct 1982 to May 1983. The wind scale is given at the bottom of the figure.

The statistically significant wind anomalies, however, are primarily associated with the Philippine Sea anticyclone (Fig. 4a). Its baroclinic structure suggests that the anomalous Philippine Sea anticyclone originates from the convective heating anomalies that are induced by tropical SST anomalies.

The direct atmospheric response to the equatorial central Pacific warming is manifested as a Matsuno (1966)–Gill (1980) pattern, namely, a pair of anomalous cyclonic equatorward winds and associated equatorial westerly anomalies (Fig. 4a). However, the Philippine Sea anticyclonic anomalies cannot be simply explained as a direct response to the central Pacific warming.

Note that the SST anomalies in the mature phase include not only the prominent equatorial eastern–central Pacific warming but also accompanying negative SST

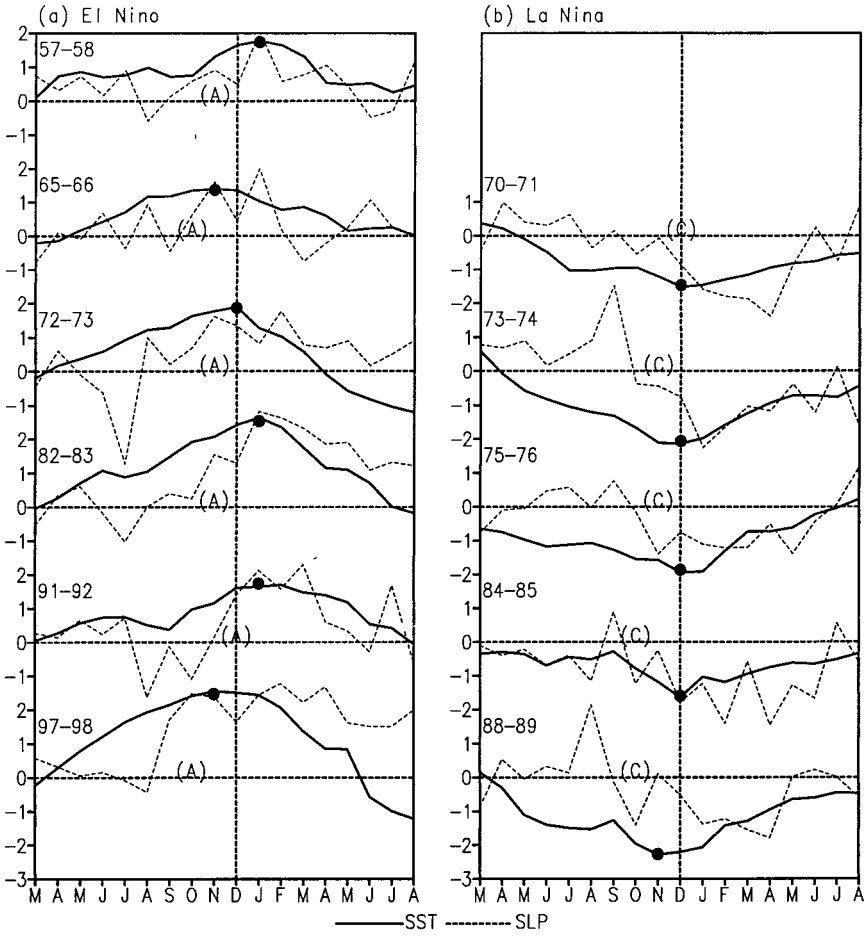

FIG. 9. Monthly mean SST anomalies (°C) at Niño-3.4 region (solid) and sea level pressure anomalies (hPa) over the Philippine Sea (10°–20°N, 120°–150°E) (dashed) during the mature phases of (a) the six warmest and (b) the five coldest episodes shown in Fig. 1. Symbols (A) and (C) indicate the timing of the rapid establishment of the anomalous Philippine Sea anticyclone (cyclone). The black dots denote the times of the warm and cold peaks.

anomalies in the western Pacific. The latter have a horseshoe shape with cooling centers located in the Philippine Sea and the southwestern Pacific around (20°S, 180°E). In the marginal seas of East Asia and the tropical Indian Ocean, there are also weak positive anomalies. The amplitude of the cooling in the western Pacific is much smaller than the warming in the equatorial eastern–central Pacific. However, its impact on the atmospheric convection should not be overlooked, because the development of convection depends on total SST (Graham and Barnett 1987). Since the mean SST in the tropical western Pacific is much higher than in the central Pacific, the atmosphere is more sensitive to the SST variation in the warm pool than in the equatorial cold tongue (Palmer and Owen 1986; Ju and Slingo 1995).

To assess the contribution of the SST anomalies in the western and eastern Pacific to the formation of the Philippine Sea wind anomalies, we first used an intermediate tropical atmospheric model originally developed by Wang and Li (1993) and improved by Fu and Wang (1999). The model is a 2½-layer, primitive-equation model. It is aimed at simulating realistic monthly mean surface winds, sea level pressure, and rainfall for specified lower-boundary conditions. The model features active interaction between the free-tropospheric flows driven by convective heating and differential longwave radiative cooling, and the boundary layer flows driven by SST gradient forcing. For a given climatological SST distribution the model is capable of reproducing realistic climatological surface winds in the Tropics (Fig. 12a). It can also produce realistic surface wind anomalies when the model is forced by specified SST anomalies (Fu and Wang 1999) and when coupled with an ocean model (Wang and Fang 2000). Although the model does not simulate midlatitude baroclinic waves, this tropical climate model is ideal for isolation of the contribution of tropical SST anomalies in forcing the Philippine Sea anticyclone.

In the benchmark experiment, the composite SST anomalies for the major warm events shown in Fig. 6a

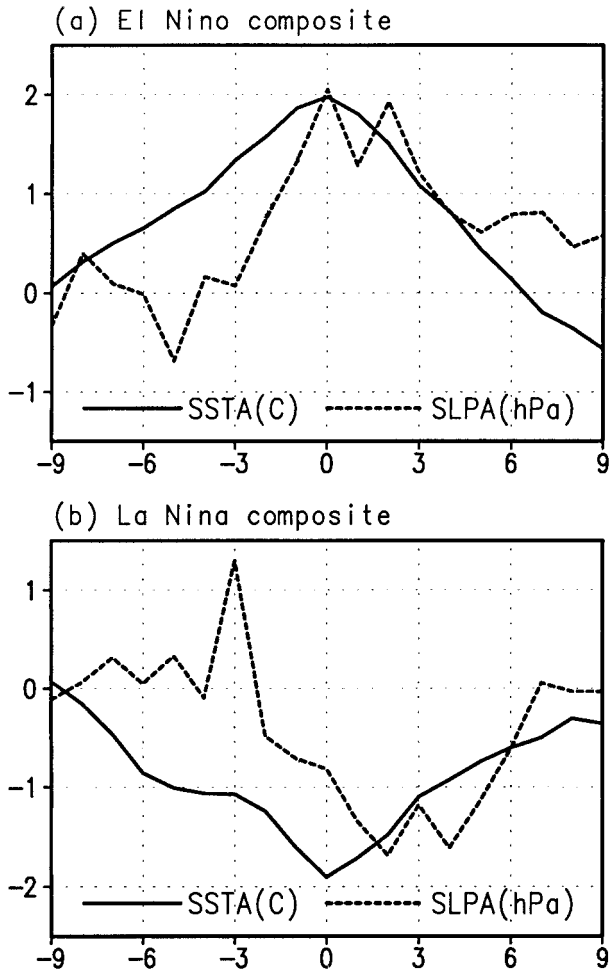

FIG. 10. Composite monthly mean SST anomalies (°C) at Niño-3.4 region (solid curves) and the sea level pressure anomalies (hPa) over the Philippine Sea (10°–20°N, 120°–150°E) (dashed curves). The composite is centered on the warm and cold peaks indicated in Fig. 9. The abscissa is the lag time (month) with respect to the warm and cold peaks (lag 0). Positive (negative) lags indicate after (before) the warm and cold peaks.

are added to the January mean SST in a domain bounded by 40°S and 40°N in latitude and 40°E and 60°W in longitude. Total SST was then used as lower-boundary forcing. The resultant anomalous surface winds were obtained from subtraction of the model climatology from the long-term mean solution forced by the total SST. The simulated anomalous winds bear qualitative similarities with the observed counterparts in the Tropics (Fig. 12b). In addition to the twin cyclonic wind stress curls residing on each side of the equator in the central Pacific, there is an anomalous anticyclone over the Philippine Sea, but it is weaker than the observed counterpart. Nevertheless, the results shown in Fig. 12b suggest that the tropical SST anomalies are partially responsible for the formation of the Philippine Sea anticyclone. The discrepancy between the model simulation and observations hints at the potential contribution of extratropical transient baroclinic waves, in particular those associated with the East Asian winter monsoon.

To determine the roles of local versus remote SST anomalies in generating the western North Pacific anticyclonic anomalies, we performed a number of controlled experiments. In the first experiment we retain only the positive SST anomalies in the eastern–central Pacific in the total SST forcing. The model shows no sign of the anomalous Philippine Sea anticyclone (Fig. 12c). On the other hand, if we retain only the negative SST anomalies in the western Pacific by removing the positive SST anomalies in the tropical Indian and Pacific Oceans, the resultant Philippine Sea anticyclonic anomalies are produced but appreciably weaker than that obtained in the benchmark experiment (Fig. 12d). This suggests that the local SST anomalies are necessary, but the remote eastern–central Pacific warming is also important for development of the Philippine anticyclone. The effects of the weak SST anomalies in the Indian Ocean and South China Sea have also been tested. Results show that they significantly affect local surface winds, but their influence on the Philippine Sea anticyclone is small.

The above assertion is further verified using the Center for Ocean–Land–Atmosphere Studies (COLA) atmospheric general circulation model (Kirtman and DeWitt 1997). This model has been tested extensively and used to forecast climate anomalies associated with ENSO (Shukla 1998). We start from a January mean state and integrate the model for 18 months by imposing time-dependent anomalous monthly mean SST anomalies on the climatological annual cycle SST. The SST anomalies are composites for the major warm events shown in Fig. 3 for the period from January of the year during which ENSO matures to June of the following year. Three experiments have been performed that are parallel to those experiments with the intermediate model.

In the benchmark experiment, the total SST anomalies in the tropical Pacific are used as time-dependent anomalous lower-boundary forcing. Figure 13c shows the boreal winter (December–February) mean SST anomalies used in the experiment. The resultant anomalous surface winds and pressure in the boreal winter are shown in Fig. 13a. In the tropical Pacific, the simulated surface pressure and wind anomalies (Fig. 13a) agree well with observations shown in Fig. 4a. The simulated Philippine Sea anticyclone is more realistic than that obtained by the intermediate model. However, the extratropical portion of the massive western North Pacific anticyclone was missed, although the cyclonic anomalies in the northeast Pacific were captured. In extratropical regions, the response is sensitive to the effects of atmospheric internal dynamics (transient baroclinic waves). Ensemble experiments are needed to better assess the extratropical response. A similar experiment using the SST anomalies from January 1982 to June 1983 was performed. The results in the Tropics are essentially the

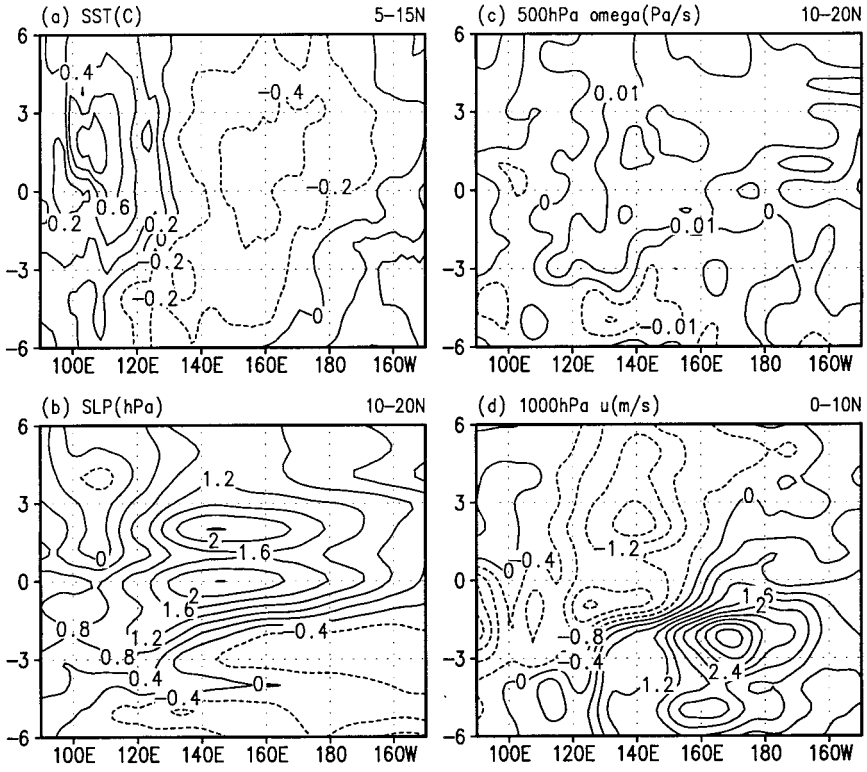

FIG. 11. Composite longitude–time diagrams of (a) SST anomalies (°C) averaged over 5°–15°N, (b) sea level pressure anomalies (hPa) averaged over 10°–20°N, (c) 500-hPa vertical pressure velocity anomalies (10^{-2} Pa s^{-1}) averaged over 10°–20°N, and (d) zonal wind anomalies (m s^{-1}) averaged over 0°–10°N for the six warmest episodes shown in Fig. 3. The vertical axis is the lag time (month) with respect to the warm and cold peaks.

same, but the midlatitude circulation anomalies are somewhat different. Nevertheless, the results shown in Fig. 13a indicate that the tropical SST anomalies are responsible for the formation of the Philippine Sea anticyclone. This anticyclone is located slightly to the northwest of the suppressed precipitation (Fig. 13b), implying that it is a Rossby wave response to the negative condensational heating anomalies in the eastern Philippine Sea.

If we impose only the eastern–central Pacific positive SST anomalies in the SST forcing (Fig. 14c), the simulation reproduces a Matsuno–Gill response in the central–eastern Pacific that is similar to that in the benchmark experiment. However, like the intermediate model, it does not reproduce the Philippine Sea anticyclone and associated high-pressure anomalies (Fig. 14a). The convection over the Philippine Sea was not suppressed due to the absence of the local cooling. This implies that the in situ cooling in the western Pacific, although weak, is necessary for generating the anticyclone in both the general circulation and the intermediate models. The Philippine Sea anticyclone, in terms of the Matsuno–Gill dynamics, is essentially a Rossby wave response to the in situ suppressed heating. Without the western Pacific cooling, the response to eastern Pacific warming is overwhelmed by the anomalous equatorial Walker cell.

If we retain only the SST anomalies in the western north Pacific (the SST anomalies in the mature phase are shown in Fig. 15c), the Matsuno–Gill pattern in the central–eastern Pacific disappears and the anomalies in the northeast and southeast Pacific extratropics also change drastically. However, the patterns of circulation and precipitation anomalies in the west Pacific (west of the date line, Figs. 15a,b) bear close similarity to those in the benchmark run (Fig. 13a,b). Quantitatively, the simulated amplitude of the Philippine Sea high-pressure and negative precipitation anomalies are only about half of those obtained in the control experiment. This indicates that in the pressence of the in situ cooling, the remote eastern–central Pacific warming also contributes considerably to the western Pacific wind and precipitation anomalies. Therefore, the atmospheric response to the local and remote forcing is nonlinear, and both are important.

Locally, the in situ cooling in the western North Pacific can effectively reduce atmospheric boundary layer temperature and humidity by cutting down latent and sensible heat exchange between the ocean and atmosphere and turbulent mixing in the boundary layer. The

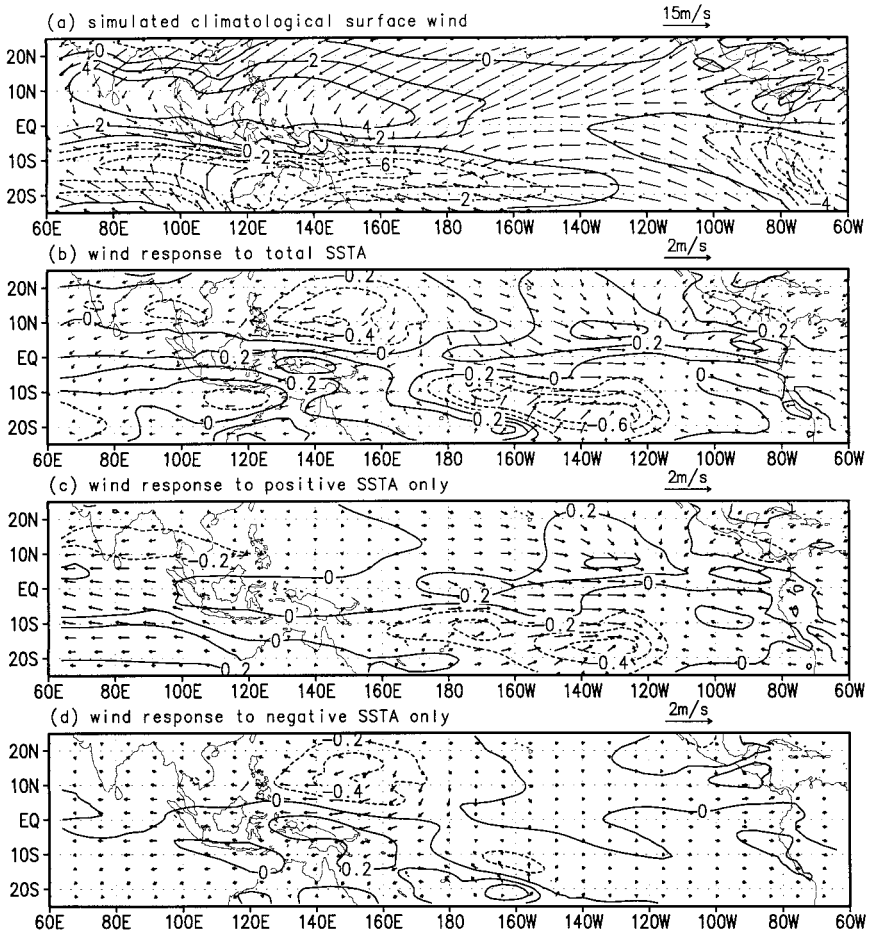

FIG. 12. Results simulated by the University of Hawaii intermediate tropical atmospheric model. (a) The simulated Jan mean surface winds and vorticity (contour in 10^{-6} s^{-1}). (b) The surface wind and vorticity (contour in 10^{-6} s^{-1}) anomalies simulated using total SST forcing (Jan mean plus the SST anomalies shown in Fig. 6a). (c) and (d) are the same as in (b), except that in (c) the lower-boundary forcing includes only the positive SST anomalies in the eastern Pacific, whereas in (d) the lower-boundary forcing contains only the negative SST anomalies in the tropical Pacific. The wind scale is given by the arrows at the top right corner.

lower-tropospheric cooling in the western Pacific can be seen from the composite 850-hPa temperature field (Fig. 6b). A decrease in the lower-troposphere temperature and humidity leads to the suppression of convective instability and an increase of surface pressure. The rise of surface pressure would induce anticyclonic vorticity and boundary layer divergence through Ekman pumping. The low-level divergence would, in turn, favor generation of anticyclonic anomalies in the subtropical latitudes (15°–20°N) where local horizontal advection of vorticity is weak. This low-level wind divergence, along with reduced convective instability, suppresses convection and promotes anomalous sinking motion, which is supported by the observed 500-hPa vertical motion field (Fig. 7a).

Remotely, the enhanced convective heating associated with the strong central Pacific warming generates upward motion in the eastern–central Pacific with compensating descending air preferably occurring over the Philippine Sea where the upper-level westerly jet favors negative potential vorticity and upper-level convergence. This is indeed the case in the model. It is also consistent with the observed upper-level velocity potential and divergent winds (Fig. 7b). The abnormal upper-level convergence over the Philippine Sea suppresses convective heating, favoring formation of a low-level anticyclonic Rossby wave cell. Thus, the central Pacific warming also contributes to the formation of the western Pacific anticyclone by enhancing a direct, thermally driven divergent circulation.

6. Discussion: The causes of Pacific–East Asian (PEA) teleconnection

The numerical experiments described in the previous section demonstrate the importance of the local cooling

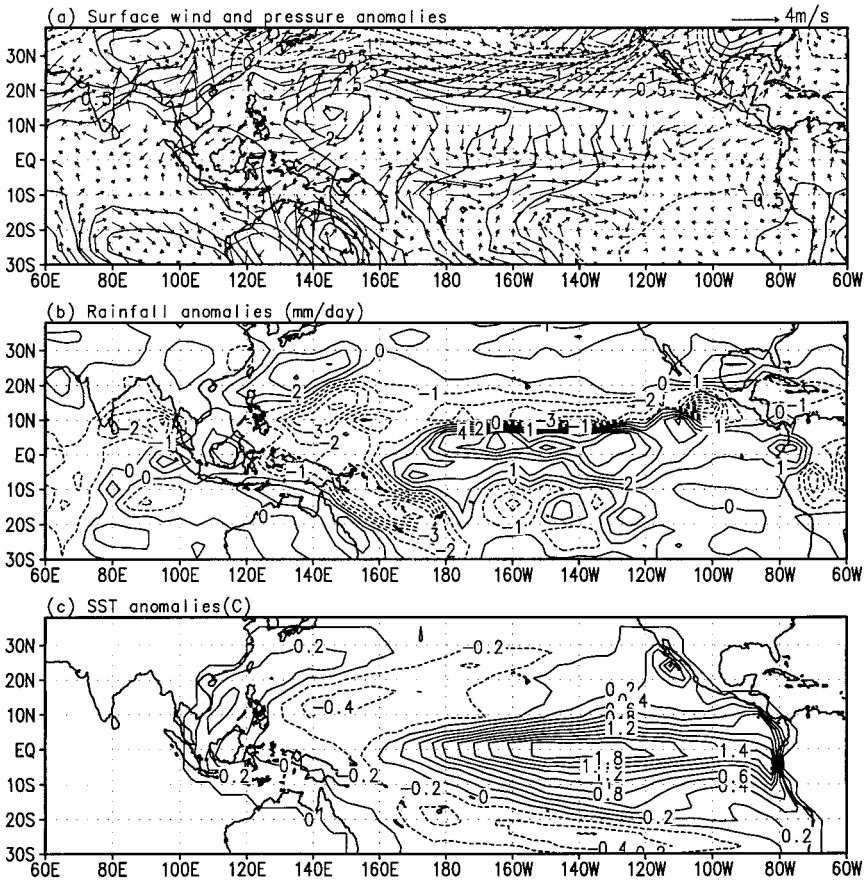

FIG. 13. (a) Surface wind and pressure anomalies and (b) rainfall anomalies during the mature phase of ENSO (Dec–Feb) simulated by the COLA atmospheric general circulation model. The model was forced by the total SST, which consists of the climatological annual cycle and the composite time-dependent SST anomalies for the six warmest episodes. (c) The composite anomalous SST used in the model during the mature phase (Dec–Feb mean).

in the establishment and maintenance of the Philippine Sea anticyclone but do not address the question of where the western Pacific cooling comes from in the first place. This section will discuss factors and processes that are critical to the development and maintenance of the WNP SST and wind anomalies.

a. The roles of the ocean–atmosphere interaction in the WNP

In theory, oceanic waves forced in the remote regions can adjust the local thermocline and the vertical displacement of the thermocline can then affect SST through vertical temperature advection. This process dominates SST variations in the eastern equatorial Pacific, because the mean thermocline there is shallow (from 50 to 100 m) and mean upwelling takes place due to the prevailing trades. In the western Pacific, however, the mean thermocline is deep (about 150 m) and the upwelling is absent. Even if the remotely forced oceanic waves were to propagate into the western Pacific and induce a significant vertical displacement, the SST would not appreciably feel it, because the vertical advection is weak due to the lack of mean upwelling and due to the great depth of the mean thermocline. For this reason, the SST variability in the warm pool regions is primarily associated with the mixed layer thermodynamics including entrainment-induced mixed layer depth variation and the surface heat flux exchange with the atmosphere. Recent Tropical Ocean–Global Atmosphere Coupled Ocean–Atmosphere Response Experiment (TOGA COARE) experiments have shown that the major processes that cause the low-frequency SST variations in the warm pool are the surface latent heat flux and the downward shortwave radiation flux (e.g., Godfrey et al. 1995; Lau and Sui 1997). Based on these observations, the primary causes of SST variations in the western Pacific are the variations in the surface wind speed and the cloud amount, which control the latent and shortwave radiation fluxes, respectively. Therefore, we infer that the change of SST in the western Pacific is primarily caused by in situ anomalous atmospheric conditions.

From an oceanographic point of view, the cooling in

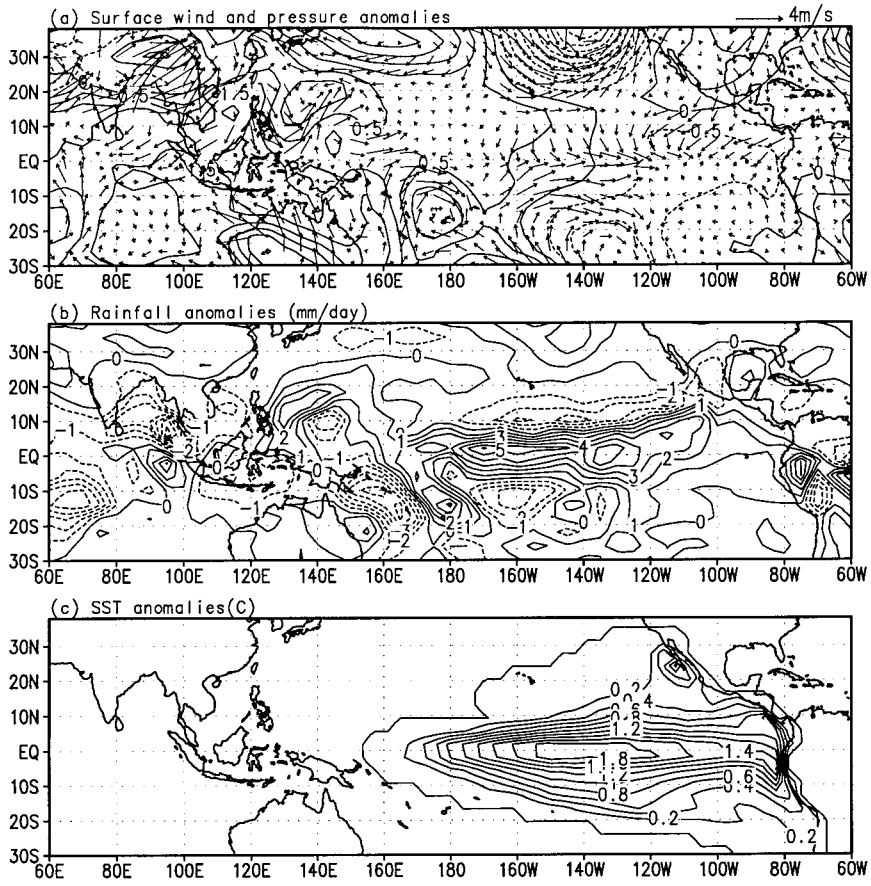

FIG. 14. The same as in Fig. 13 except that the anomalous SST forcing includes eastern-central Pacific positive SST anomalies only.

the western North Pacific is primarily caused by in situ anomalous atmospheric conditions. From an atmospheric perspective, however, the key system of the Pacific–East Asian teleconnection, the Philippine Sea anomalous anticyclone, is a Rossby wave response to the in situ cooling of the ocean surface. The circular argument here implies that *the formation and maintenance of the Pacific–East Asian teleconnection result from ocean–atmosphere interaction.*

After the rapid development, the WNP anticyclonic (cyclonic) anomalies and the associated equatorial easterly (westerly) anomalies persist for two or three seasons (Figs. 9 and 10). Sometimes these anomalies can survive even after the remote atmospheric forcing from the central Pacific warming wanes. This suggests that WNP wind anomalies are not predominately maintained by the equatorial central Pacific warming. This assertion is consistent with our model results shown in Figs. 12–15. Because of the chaotic nature of the atmospheric motion, the atmosphere alone cannot provide a long-term memory. Thus, such persistent atmospheric anomalies are likely maintained by local atmosphere–ocean interaction.

How can air–sea interaction amplify and maintain the atmospheric anomalies? We propose that a positive feedback between the anticyclone (cyclone) and the sea surface cooling (warming) plays a critical role. Comparison of Figs. 11a and 11b reveals that the low-level anticyclone is located about 20° longitude to the west of the cooling region. This phase shift is also clearly reflected in the composite horizontal structure (Figs. 5a and 6a) and in the 1982/83 event shown in Fig. 8. It is confirmed by the results of numerical model simulations shown in Figs. 12b and 13a. This phase shift is a robust feature and is critical for the positive feedback between the anticyclone and negative SST anomalies. The idea is illustrated by the schematic diagram in Fig. 16 and explained as follows. Over the Philippine Sea, the mean winds (basic states) are dominated by the northeasterly trade winds in the cold season from October to May. To the east of an anomalous anticyclone, the total wind speed and associated evaporation and entrainment cooling is enhanced. The wind-induced SST variation would favor mixed-layer cooling ahead of the anticyclone. The negative SST anomaly located east of the anomalous anticyclone, in turn, favors amplification of the anomalous anticyclone by exciting Rossby waves. Therefore, the positive feedback between the anticyclonic wind and

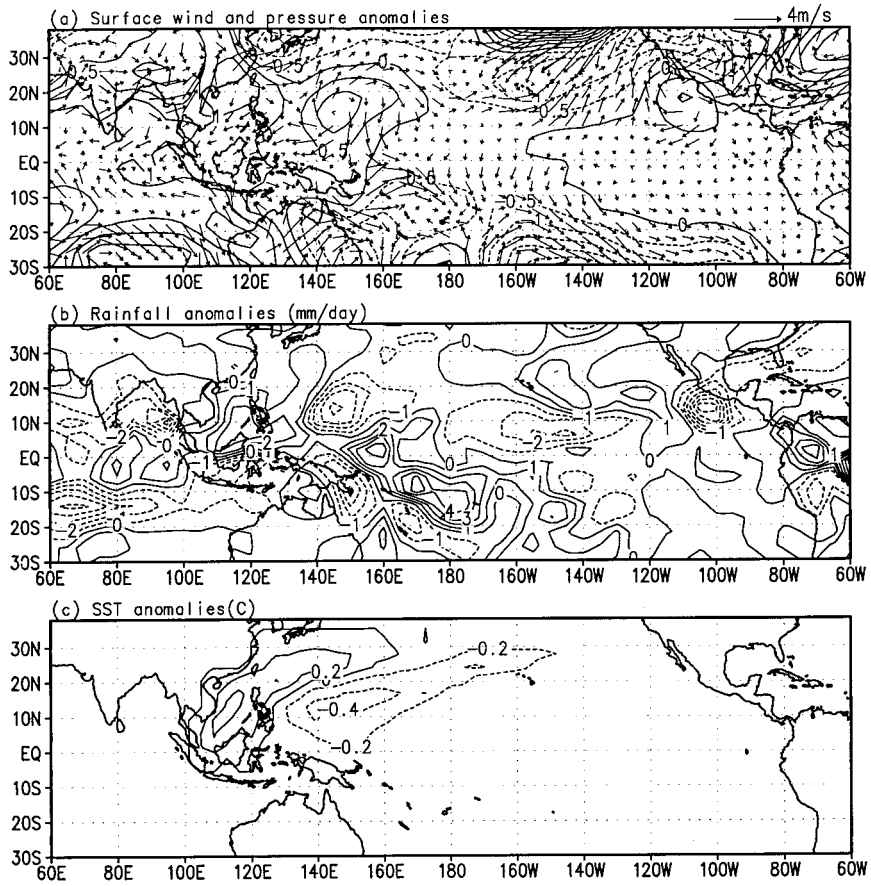

FIG. 15. The same as in Fig. 13 except that the anomalous SST forcing includes the western North Pacific negative SST anomalies only.

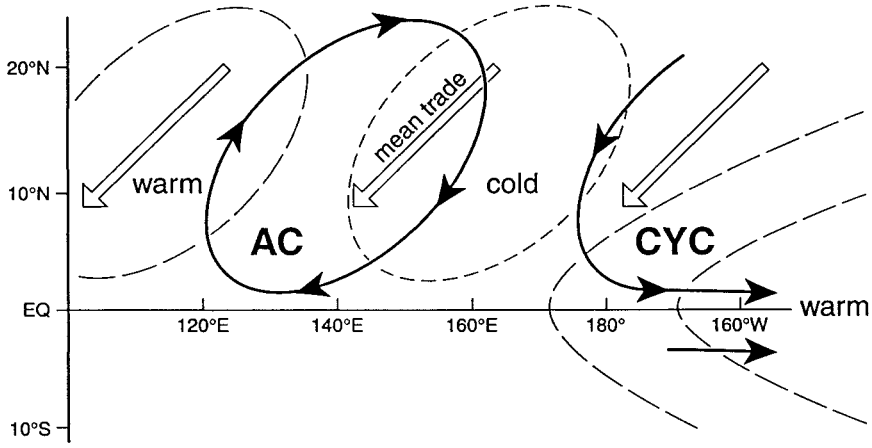

FIG. 16. Schematic diagram showing the air–sea interaction in the western North Pacific that maintains the Philippine Sea anticyclonic anomalies and associated negative SST anomalies in the western North Pacific. The double arrows denote the mean trade winds. The heavy lines with black arrows represent the anomalous winds. The long (short) dashed lines indicate contours of positive (negative) SST anomalies.

SST through evaporation and entrainment processes in the western Pacific may play a critical role in the development and maintenance of the western Pacific surface wind and SST anomalies against thermal dissipation.

b. The roles of the central Pacific warming

While the positive feedback between the anticyclone and sea surface cooling may play critical roles, it by no means implies that the formation of the WNP wind anomalies is independent of the ENSO warming. The numerical experiments described in section 5 show that, without including the central Pacific warming, the Philippine Sea anticyclone does not fully develop. The strength reaches only about one-half that obtained with the forcing from the central Pacific warming. More importantly, the formation of the WNP SST and wind anomalies depends on the central Pacific warming in a number of ways.

The central Pacific warming induces equatorward flows to the west of the warming, which are connected with the equatorial westerly anomalies near the date line (Fig. 4a and 16). The equatorward wind anomalies in the Northern Hemisphere are superposed on the mean northeast trades, increasing the total wind speed and, thus, the evaporational cooling in the western North Pacific. The cooling of the sea surface would, in turn, induce an anticyclone to the westward and poleward side of the cooling regions over the Philippine Sea due to a Rossby wave response to the suppressed convective heating.

The warming in the central Pacific also sets up a favorable large-scale environment for the effective WNP air–sea interaction, which is critical for the sudden establishment and maintenance of the Philippine Sea anticyclone. The Pacific–East Asian teleconnection is derived from major El Niño and La Niña episodes. The Philippine Sea anticyclone did not develop or occurred only briefly but did not persist during some moderate events (e.g., 1968/69, 1976/77, 1993/94) and the 1986/87 event. An important feature in these four events is the insufficient strength of the central Pacific warming (the 3-month running mean Niño-3.4 SST anomalies less than 1°C) toward the end of the ENSO development year (figure not shown). This suggests that the strong warming in the central Pacific is an important precondition for the development of the Philippine Sea anticyclone. Why is this so?

The establishment of the anticyclone over the WNP is normally rapid, often taking only 1 month (Figs. 8 and 9). The rapid establishment of the Philippine Sea anticyclone and strengthening of the local cooling imply that the air–sea interaction occurs rapidly. Therefore, it may be triggered by atmospheric processes. The sudden rise of the pressure in the western North Pacific may be initiated by strong synoptic or intraseasonal events. A strong cold surge, for instance, can cool ocean surfaces by half a degree on a timescale of one week. This has been observed during the TOGA COARE intensive observation period over the equatorial western Pacific warm pool (e.g., Sui et al. 1997). The normal path of the cold surge intrusion to low latitudes occurs over the South China Sea. Intrusion of cold surges into the Philippine Sea and western North Pacific requires an eastward shift of the westerly jet. The central Pacific warming causes such a shift. It enhances the subtropical anticyclone and induces an eastward shift and intensification of the Aleutian low and associated westerly jet (the PNA pattern). Associated with the eastward shift of the Aleutian low, the pressure rises east of Japan (Fig. 4). This anomalous large-scale circulation favors intrusion of cold surges into the Philippine Sea. Thus, the central Pacific warming sets up an environment that is conducive for the effective air–sea interaction in the WNP. The latter leads to the rapid development of the western Pacific cooling and the Philippine Sea anticyclone.

In summary, the central Pacific warming plays an essential role in the formation of the western Pacific cooling and the Philippine Sea anomalous anticyclone by setting up a favorable environment for the air–sea interaction and the tropical–extratropical interaction.

7. Summary

The Pacific–East Asian teleconnection is a mechanism that links central Pacific SST anomalies with East Asian climate variations. It displays two distinctive features in comparison with the PNA teleconnection. The former is confined to the lower troposphere while the latter are most evident in the upper troposphere. The former is a vorticity wave pattern that emanates from the equatorial central Pacific *westward* and poleward against the westerly jet stream, whereas the latter emanate *eastward* and poleward down the boreal winter westerly jet stream.

The mechanisms responsible for the Pacific–East Asian teleconnection also differ fundamentally from those for the Pacific–North American teleconnection. A key system that bonds the equatorial central Pacific warming (cooling) and weak (strong) East Asian winter monsoon is the large-scale western North Pacific anomalous anticyclone (cyclone). The analysis of the observed structures and evolution reveal that the Philippine Sea wind anomalies are originated and maintained by a positive feedback resulting from the thermodynamic coupling of the atmospheric Rossby waves and the oceanic mixed layer in the presence of strong remote forcing from the equatorial eastern–central Pacific. The cooling in the western Pacific and the warming in the East Asian marginal seas also results from this interaction.

There is, however, a possible linkage between the PNA and PEA teleconnection. Figure 4 shows that the massive western North Pacific anticyclone integrates two anticyclonic circulation cells, one centered in the

Philippine Sea (15°N, 140°E) and the other centered east of Japan (40°N, 170°E). The two anticyclonic gyres exhibit different vertical structures. The Philippine Sea anticyclone is essentially baroclinic, and the anticyclone in the Kuroshio extension region contains a considerable barotropic component. This suggests that the Philippine Sea anticyclone is likely stimulated by the anomalous tropical heating, and the extratropical portion of the anticyclone is plausibly associated with midlatitude dynamical instability similar to the PNA dynamics. During ENSO warming, the anticyclonic anomalies in the Kuroshio extension and the cyclonic anomalies in the northeastern Pacific (Fig. 4) reflect the southeastward shift of the Aleutian low and eastward extension of the East Asian cold high (figure not shown). The extratropical portion of the anomalous western North Pacific anticyclone may be a manifestation of the anomalies associated with the PNA teleconnection.

We speculated that the formation of the western North Pacific lower-tropospheric anticyclone is primarily linked to the Pacific SST anomalies because the anomaly signals decay poleward and westward toward the Asian continent. The fact that the teleconnection can be reproduced in the absence of the winter monsoon supports this point of view. However, Asian winter monsoon variability can have considerable impacts on the formation and maintenance of the Pacific–East Asian teleconnection through the *interaction between extratropical and tropical circulations.* A previous study of the relationship between the East Asian winter monsoon and equatorial convection (Chang and Lau 1982) has shown evidences of such an interaction. Tropical–extratropical interaction may serve as a catalyst for the western Pacific air–sea interaction in establishing the PEA teleconnection. The simultaneous establishments of the Philippine Sea wind anomalies and SST anomalies also suggest the potential contribution of the extratropical–tropical interaction through intrusion of cold air into the Philippine Sea. Such an abnormal path of cold surge is possible in the presence of strong warming in the equatorial central Pacific.

Because the thermodynamic coupling between atmospheric Rossby waves and ocean mixed layer temperature variation depends on the boreal winter mean surface winds, the development and maintenance of the western Pacific wind and SST anomalies are favored in the boreal cold season from late fall to spring. This seasonal dependence may partially explain the observed asymmetry (with regard to the equator) in response to the ENSO warming shown in Fig. 4a. The western North Pacific anticyclonic anomaly is stronger than its southern counterpart. In a separate paper (Wang et al. 1999), we show that the Philippine Sea wind anomalies not only provide a linkage between tropical SST anomalies and the upstream extratropical climate but also contribute to ENSO turnabouts.

The persistent WNP anomalies have a profound impact on the spring rainy season in the East Asian frontal zone. The anomalies sometimes survive into early summer and affect the rainfall in the East Asian subtropical front (Mei-yu or Baiu). This assertion involves certain degrees of uncertainty and calls for further investigation.

The potentially important off-equatorial air–sea interaction processes in the western Pacific have not been properly monitored and simulated by coupled ocean–atmospheric models. To demonstrate the roles of the air–sea interaction in generation and maintenance of the Pacific–East Asia teleconnection requires a time-dependent calculation with a coupled atmosphere–ocean model. Much research is needed in this regard to further our understanding of the dynamics of ENSO and teleconnection.

Acknowledgments. The authors thank Drs. Shukla and Kinter for kindly providing the COLA model and appreciate discussions with Dr. R. Lukas and comments from Dr. T. A. Schroeder and Mr. C. Orndorff. This research project is supported by NOAA Cooperative Agreement Number NA67RJ0154, NSF Climate Dynamics Program (Grant ATM-9613776), and ONR Marine Meteorology Program.

REFERENCES

Bjerknes, J., 1966: A possible response of the atmospheric Hadley circulation to equatorial anomalies of ocean temperature. *Tellus,* **18,** 820–829.

——, 1969: Atmospheric teleconnections from the equatorial Pacific. *Mon. Wea. Rev.,* **97,** 163–172.

Chang, C.-P., and K.-M. Lau, 1982: Short-term planetary-scale interactions over the Tropics and midlatitudes during northern winter. Part I: Contrasts between active and inactive periods. *Mon. Wea. Rev.,* **110,** 933–946.

Chen, L., M. Dong, and Y. Shao, 1992: The characteristics of interannual variation on the East Asian monsoon. *J. Meteor. Soc. Japan,* **70,** 397–421.

Fu, C., and X. Teng, 1988: The relationship between ENSO and climate anomaly in China during the summer time (in Chinese). *Sci. Atmos. Sinica,* Special Issue, 133–141.

Fu, X., and B. Wang, 1999: On the role of longwave radiation and boundary layer thermodynamics in forcing tropical surface winds. *J. Climate,* **12,** 1049–1069.

Gill, A. E., 1980: Some simple solutions for heat-induced tropical circulation. *Quart. J. Roy. Meteor. Soc.,* **106,** 447–462.

Godfrey, S. P., and Coauthors, 1995: Surface fluxes and mixed layer heat and freshwater budgets in TOGA COARE. *Proc. Int. Scientific Conf. on the Tropical Ocean Global Atmosphere Program,* Melbourne, Australia, World Meteorological Organization, 464–468.

Graham, N. E., and T. P. Barnett, 1987: Sea surface temperature, surface wind divergence, and convection over tropical oceans. *Science,* **238,** 657–659.

Horel, J. D., and J. M. Wallace, 1981: Planetary-scale atmospheric phenomena associated with the Southern Oscillation. *Mon. Wea. Rev.,* **109,** 813–829.

Hoskins, B. J., and D. J. Karoly, 1981: The steady linear response of a spherical atmosphere to thermal and orographic forcing. *J. Atmos. Sci.,* **38,** 1179–1196.

Huang, R., and L. Lu, 1989: Numerical simulation of the relationship between the anomaly of subtropical high in East Asia and the convective activities in the tropical western Pacific. *Adv. Atmos. Sci.,* **6,** 202–214.

Ji, L., S. Sun, and K. Arpe, 1997: Model study on the interannual

variability of Asian winter monsoon and its influence. *Adv. Atmos. Sci.,* **14,** 1–22.
Ju, J., and J. M. Slingo, 1995: The Asian summer monsoon and ENSO. *Quart. J. Roy. Meteor. Soc.,* **121,** 1133–1168.
Kalnay, E., and Coauthors, 1996: The NCEP/NCAR 40-Year Reanalysis Project. *Bull. Amer. Meteor. Soc.,* **77,** 437–471.
Kang, I., and Y. Jeong, 1996: Association of interannual variations of temperature and precipitation in Seoul with principal modes of Pacific SST. *J. Korean Meteor. Soc.,* **32,** 339–345.
Kirtman, B. P., and D. G. DeWitt, 1997: Comparison of atmospheric model wind stress with three different convective parameterizations: Sensitivity of tropical Pacific Ocean simulations. *Mon. Wea. Rev.,* **125,** 1231–1250.
Lau, K.-M., 1992: The East Asian summer monsoon rainfall variability and climate teleconnection. *J. Meteor. Soc. Japan,* **70,** 211–241.
——, and M. Li, 1984: The monsoon of East Asia and its global association—A survey. *Bull. Amer. Meteor. Soc.,* **65,** 114–125.
——, and C.-H. Sui, 1997: Mechanisms of short-term sea surface temperature regulation: Observations during TOGA COARE. *J. Climate,* **10,** 465–472.
Liu, T., W. Tang, and H. Hu, 1998: Spaceborne sensors observe El Niño's effects on ocean and atmosphere in North Pacific. *Eos, Trans. Amer. Geophys. Union,* **79,** 249–252.
Matsuno, T., 1966: Quasi-geostrophic motion in the equatorial area. *J. Meteor. Soc. Japan,* **44,** 25–43.
Nitta, T., and Z.-Z. Hu, 1996: Summer climate variability in China and its association with 500 hPa height and tropical convection. *J. Meteor. Soc. Japan,* **74,** 425–445.
Palmer, T. M., and J. A. Owen, 1986: A possible relationship between some ''severe'' winters in North America and enhanced convective activity over the tropical west Pacific. *Mon. Wea. Rev.,* **114,** 648–651.
Rasmusson, E. M., and T. H. Carpenter, 1982: Variations in tropical sea surface temperature and surface wind fields associated with the Southern Oscillation/El Niño. *Mon. Wea. Rev.,* **110,** 354–384.
Ropelewski, C. F., and M. S. Halpert, 1987: Global and regional scale precipitation patterns associated with the El Niño/Southern Oscillation. *Mon. Wea. Rev.,* **115,** 1606–1626.
——, and ——, 1989: Precipitation patterns associated with the high index phase of the Southern Oscillation. *J. Climate,* **2,** 268–284.
——, and ——, 1996: Quantifying Southern Oscillation–precipitation relationships. *J. Climate,* **9,** 1043–1059.
Shen, S., and K.-M. Lau, 1995: Biennial oscillation associated with the East Asian summer monsoon and tropical sea surface temperature. *J. Meteor. Soc. Japan,* **73,** 105–124.
Shukla, J., 1998: Predictability in the midst of chaos: A scientific basis for climate forecasting. *Science,* **282,** 728–731.
Simmons, A. J., J. M. Wallace, and G. W. Branstator, 1983: Barotropic wave propagation and instability, and atmospheric teleconnection patterns. *J. Atmos. Sci.,* **40,** 1363–1392.
Sui, C.-H., X. Li, K.-M. Lau, and D. Adame, 1997: Multiscale air–sea interactions during TOGA COARE. *Mon. Wea. Rev.,* **125,** 448–462.
Tao, S., and Q. Zhang, 1998: Response of the East Asian summer monsoon to ENSO events (in Chinese). *Sci. Atmos. Sinica,* **22,** 399–407.
Tomita, T., and T. Yasunari, 1996: Role of the northeast winter monsoon on the biennial oscillation of the ENSO/monsoon system. *J. Meteor. Soc. Japan,* **74,** 399–413.
Torrence, C., and P. J. Webster, 1998: The annual cycle of persistence in the El Niño–Southern Oscillation statistics. *Quart. J. Roy. Meteor. Soc.,* **124,** 1985–2004.
Wallace, J. M., and D. S. Gutzler, 1981: Teleconnections in the geopotential field during the Northern Hemisphere winter. *Mon. Wea. Rev.,* **109,** 784–812.
Wang, B., 1995a: Interdecadal changes in El Niño onset in the last four decades. *J. Climate,* **8,** 267–285.
——, 1995b: Transition from a cold to a warm state of the El Niño–Southern Oscillation cycle. *Meteor. Atmos. Phys.,* **56,** 17–32.
——, and T. Li, 1993: A simple tropical atmosphere model of relevance to short-term climate variations. *J. Atmos. Sci.,* **50,** 260–284.
——, and Z. Fang, 2000: Impact of the solar radiation forcing on ENSO as revealed from an intermediate coupled ocean–atmosphere model. *Climate Dyn.,* in press.
——, R. Wu, and R. Lukas, 1999: Roles of the western North Pacific wind variation in thermocline adjustment and ENSO phase transition. *J. Meteor. Soc. Japan,* **77,** 1–16.
Wang, J.-T., and J.-W. Hwu, 1994: Springtime East Asia large scale characteristics post ENSO. Part I: The spatial distribution of SST and OLR. *Atmos. Sci.,* **22,** 339–360.
Webster, P. J., V. O. Magana, T. N. Palmer, T. A. Tomas, M. Yanai, and T. Yasunari, 1998: Monsoons: Processes, predictability, and prospects for prediction. *J. Geophys. Res.,* **103,** 14 451–14 510.
Woodruff, S. D., R. J. Slutz, R. L. Jenne, and P. M. Steurer, 1987: A Comprehensive Ocean-Atmosphere Data Set. *Bull. Amer. Meteor. Soc.,* **68,** 1239–1250.
Xie, P., and P. A. Arkin, 1997: Global precipitation: A 17-year monthly analysis based on gauge observations, satellite estimates, and numerical model outputs. *Bull. Amer. Meteor. Soc.,* **78,** 2539–2588.
Yasunari, T., 1991: The monsoon year—A new concept of the climatic year in the Tropics. *Bull. Amer. Meteor. Soc.,* **72,** 937–957.
Zhang, R., A. Sumi, and M. Kimoto, 1996: Impact of El Niño on the East Asian monsoon: A diagnostic study of the '86/87 and '91/92 events. *J. Meteor. Soc. Japan,* **74,** 49–62.